DOI: 10.1002/ejoc.201000732

Nonbonded Interactions Tune Selectivities in Cycloadditions to 2,3-Dioxabicyclo[2.2.2]oct-5-ene

Paolo Quadrelli,*[a] Silvano Romano,[b] and Pierluigi Caramella*[a]

Dedicated to Prof. Rolf Huisgen on the occasion of his 90th birthday

Keywords: Facial selectivity / Density functional calculations / Cycloaddition / Osmilation / Regioselectivity

The facial selectivity of 2,3-dioxabicyclo[2.2.2]oct-5-ene in cycloaddition reactions is distressingly variable and akin to that of 2-oxa-3-azabicyclo[2.2.2]oct-5-ene derivatives. Osmilation takes place on the face *anti* to the dihetero bridge, while cycloaddition of butadiene affords exclusively the *syn* cycloadduct. Nitrile oxides add unselectively. B3LYP/LANL2DZ calculations of cycloadditions to 2,3-dioxabicyclo-[2.2.2]oct-5-ene reproduce well the experimental selectivities and give insights into the origin of the changes. The double bonds of the olefins are moderately pyramidalized toward the *anti* space, implying a preferred *anti* addition. This natural predisposition to *anti* addition is tuned by the mutual interaction between the addends. On going from osmilation to nitrile oxide and butadiene cycloadditions, the steric effects between the addend and the dimethylene bridge of the olefin increase remarkably and affect the attacking angle Θ and the tilting angle α of the *anti* addition, enforcing enhanced deformations of the olefin, which almost offset its natural *anti* predisposition. In the case of butadiene, the residual part of the steric effect increases further the *anti* barrier leading to a neat reversal of selectivity. 2,3-Dioxabicyclo[2.2.1]hept-5-ene shows a larger *anti* pyramidalization, which is akin to that of norbornene itself and to 2-oxa-3-azabicyclo[2.2.1]hept-5-ene derivatives, and mutual steric interactions have only a subordinate influence on selectivity.

Introduction

The hetero-Diels–Alder (HDA) cycloadducts **1**, readily available from nitroso carbonyl compounds and cyclic dienes, display a remarkable synthetic potential, allowing for the flexible introduction of multifunctionality.[1] The unsaturated moiety can be elaborated in a variety of ways, while the *N*-acyl substituent can be detached under mild conditions, and the cleavage of the N–O bond can be selectively performed with various reductive agents.

Among the synthetic elaborations, cycloaddition reactions to the double bond of HDA adducts **1** have been widely investigated. The *N*-acyl-2-oxa-3-azanorbornenes **1a** (n = 1) derived from the HDA cycloaddition of nitroso carbonyl compounds to cyclopentadiene are quite reactive and afford the *exo* adducts in 1,3-dipolar cycloadditions by exclusive attack of the 1,3-dipoles to dipolarophiles on the face *anti* to the dihetero bridge. The exceptionally high reactivity and exclusive *exo* selectivity of the cycloadditions is akin to that of the related parent carbocyclic norbornene, which add all types of reactants only on the *exo* face.[2] The origin of the norbornene selectivity has attracted a great deal of attention,[3] and is usually attributed to relief of strain,[4] geometric deformation of the double bond (pyramidalization due to torsional and hyperconjugative effects)[5] as well as favourable staggering effects in the *exo* attack.[6] Thus, dihydroxylation of **1a** with buffered permanganate or OsO_4/NMO[7] provides access to the *exo cis*-diols **2**, which are valuable intermediates in the total synthesis of natural products and carbocyclic nucleosides (Scheme 1). In cycloadditions with nitrile oxides only the *exo* attack is observed, and the two *exo* regioisomeric cycloadducts **3** and **4** are formed in comparable amounts due to the similar electron-

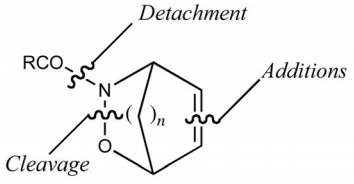

1	n	R
a	1	
b	2	
A		Ph

[a] Dipartimento di Chimica Organica, Università degli Studi di Pavia,
Viale Taramelli 10, 27100 Pavia, Italy
Fax: +39-0382-987323
E-mail: paolo.quadrelli@unipv.it
[b] Unità di Ricerca CNISM e Dipartimento di Fisica "A. Volta", Università degli Studi di Pavia,
Via A. Bassi 6, 27100 Pavia, Italy

Supporting information for this article is available on the WWW under http://dx.doi.org/10.1002/ejoc.201000732.

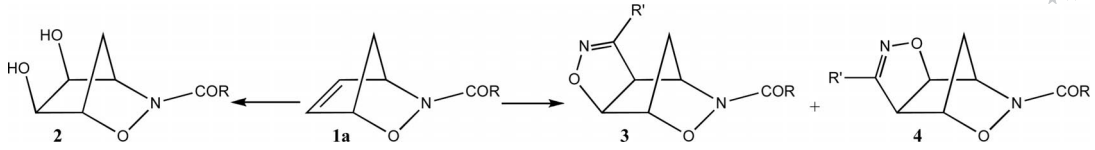

Scheme 1.

withdrawing abilities of the alkoxy and acylamino groups, whose effects are quantified by their σ_I substituent constants.[8]

At variance with **1a**, the 2-oxa-3-azabicyclo[2.2.2]oct-5-enes **1b** (n = 2) are somewhat less reactive because of the reduced strain relief[4] as well as imperfect staggering for additions on both faces which are akin to the *endo* attacks to **1a** and to norbornene itself. As far as facial selection is concerned, derivatives **1b** display a distressingly variable selectivity. Osmilation still takes place only on the face *anti* to the dihetero bridge, affording the *anti cis*-diols **5**, which are valuable intermediates in synthetic applications.[9] On the other hand, **1b** adds butadiene in a Diels–Alder (DA) reaction affording exclusively the *syn* adducts **6**.[10] We recently investigated the cycloaddition of benzonitrile oxide (BNO) to **1bA**, and obtained a mixture of all the possible regio- and stereoisomers **7**–**10** in comparable amounts[11] (Scheme 2). A similar unselective outcome was reported by Miller in the cycloaddition of benzyl azide to the *N*-Boc derivative of **1b** (R = O*t*Bu).[12] The lack of regiochemical control could be conceivably related to the similar electron-withdrawing abilities of the alkoxy and acylamino allylic substituents, but the lack of stereoselective control is less obvious because the widely different π/σ* and π/σ interactions acting on the two faces led to a deformation of the double bond, which pyramidalizes in the unsymmetrical environment.[3,5]

In calculations at the B3LYP/6-31G* level, the ground-state (GS) geometries of *N*-formyl-2-oxa-3-azabicyclo[2.2.2]-oct-5-ene **1b** (R = H) and the simpler 2,3-dioxabicyclo[2.2.2]oct-5-ene **11** show a small but significant (vide infra) pyramidalization of the double bond toward the *anti* space implying an easier *anti* attack (Figure 1), which admirably fits the osmilation results. The related 2-oxa-3-azabicyclo[2.2.1]hept-5-enes **1a** and the 2,3-dioxa derivative **12** show much larger pyramidalizations.

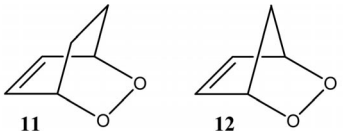

A comparison[11] of the out-of-plane tilting angles α of the vinyl hydrogen atoms in the GS geometries of dioxa and oxaaza derivatives of bicyclooctene and norbornene points out that the modest pyramidalization ($\alpha \approx 2°$) of the 2,3-dioxa- and *N*-formyl-2-oxa-3-azabicyclo[2.2.2]oct-5-enes can be related to the conflicting effects of the π/σ* and π/σ allylic interactions. The best allylic acceptors are the σ* C–X bonds of the dihetero bridge and favour *anti* pyramidali-

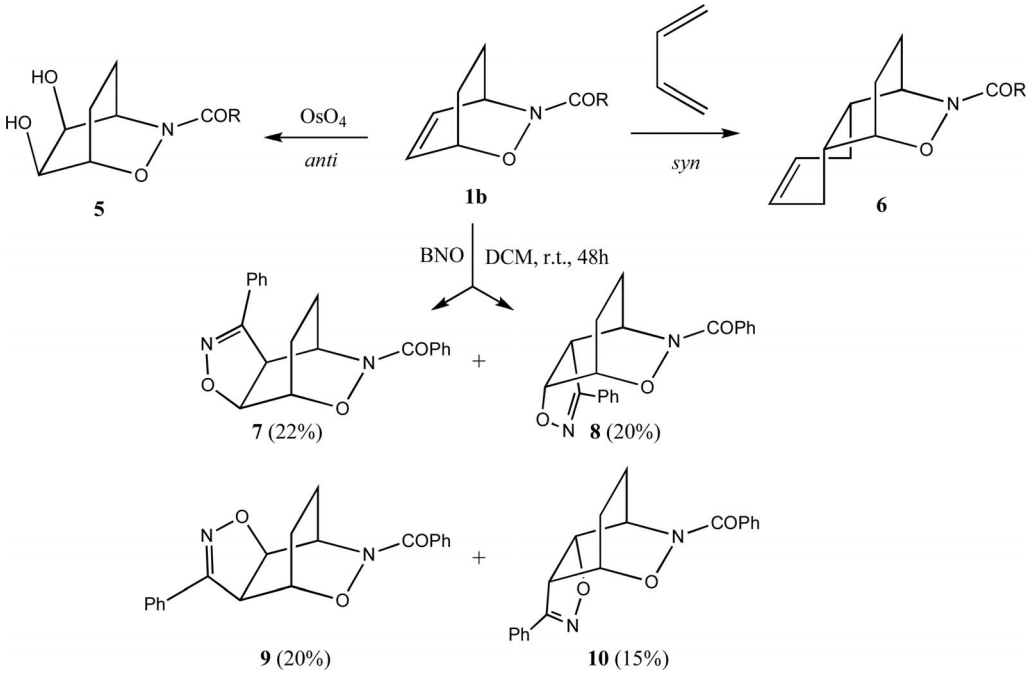

Scheme 2.

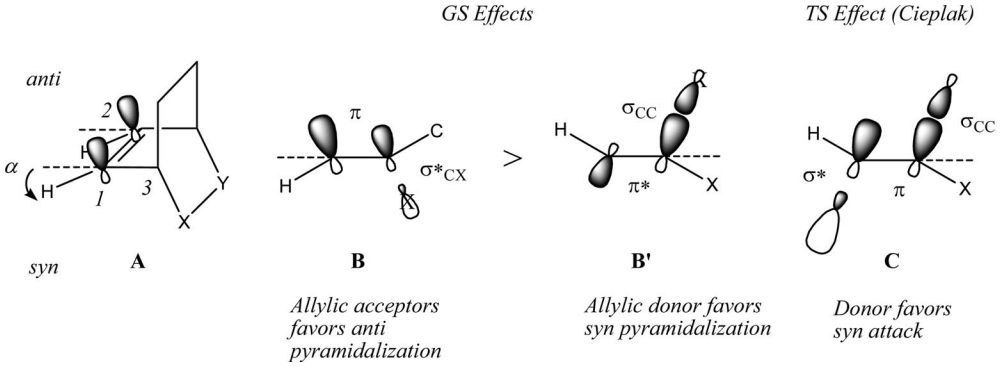

Figure 1. Pyramidalization of the double bond in *N*-formyl-2-oxa-3-aza- and 2,3-dioxabicyclo[2.2.2]oct-5-ene derivatives (A) by tilting of the vinyl hydrogen atoms out of the 1,2,3 plane. Effect of π/σ* stabilization (B) and π/σ repulsion (B′) in the interaction of π and allylic bonds. The Cieplak TS model (C) states that addition takes place on the face opposite to the best donor (i.e. *syn* to the dihetero bridge in the case of **1b**) because of the stabilizing interaction between the best σ donor and forming the σ* incipient bond.

zation as shown in part B of Figure 1. The best allylic donors are the σ C–C bonds of the dimethylene bridge, and they promote *syn* pyramidalization (B′). The net effect is the modest *anti* pyramidalization due to the larger influence of the π/σ* interactions, depicted as B > B′. The norbornene derivatives show larger pyramidalization effects ($\alpha \approx 6–7°$) since only the allylic bonds of the two-membered bridge are properly aligned for interaction with the π orbital. The two π/σ* and π/σ interactions then reinforce each other, causing the large *exo* pyramidalization, which accounts for the exclusive *exo* selectivity observed with norbornene and its 2,3-dioxa and 2-oxa-3-aza derivatives.

Transition-state (TS) effects can change the intrinsic GS preference of the dipolarophiles. The widely quoted Cieplak effect[13] shown in part C of Figure 1 states that additions take place *anti* to the best donor, accounting for the outcome of many DA cycloadditions.[14] In the case of the 2,3-dioxa- and 2-oxa-3-azabicyclo[2.2.2]oct-5-enes, the Cieplak effect predicts a *syn* addition and would admirably account for the *syn* additions of butadiene to **1b**. Clearly, the cases of the cycloaddition of BNO and benzyl azide to **1b** fall in between and would require a composition of GS and TS effects. While appealing, this simple rationalization rests upon the Cieplak TS effect, whose validity is rather controversial.[15]

In order to gain deeper insights into the origin of the variable selectivities of the cycloaddition reactions to **1b** as well as into the reliability and limitations of the GS and TS effects discussed above, we report here a theoretical study of the cycloadditions of $OsO_4 \cdot NH_3$, BNO and butadiene to 2,3-dioxabicyclo[2.2.2]oct-5-ene **11** as a simple and symmetrical model of the 2-oxa-3-azabicyclo[2.2.2]oct-5-enes **1b**. Despite the differences between **1b** and **11**, the modeling of the unsymmetrical oxaazabicyclo derivative **1b** with the symmetrical dioxa derivative **11** rests upon the almost identical pyramidalizations of their double bonds ($\alpha \approx 2°$) and the lack of a significant regiochemical effect in the attack of BNO and benzyl azide to the two different faces of **1b**. This lack of specificity is attributable to the similar σ_I substituent constants of the alkoxy and acylamino groups. Moreover, the known cycloaddition chemistry of **11**[16] shows an overall similarity to that of **1b**. Osmilation of **11** takes place exclusively *anti*.[16a] The cycloaddition of BNO is rather unselective affording the *anti* and *syn* cycloadducts in a ratio 2:1 while the *syn* attack becomes slightly preferred with bulkier nitrile oxides, nitrones and diazoalkanes.[16b]

For sake of comparison, the related cycloadditions to 2,3-dioxabicyclo[2.2.1]heptene **12** (a model of **1a**) are also reported. Only a few addition reactions have been reported for the labile **12**. A well-known example is the transfer reaction with dideuterio diimide, which takes place exclusively on the *anti* face of **12**, while **11** undergoes both *anti* and *syn* attacks.[17]

Methods

The calculations were performed with the Gaussian 03 program.[18] Geometries for all the stationary structures were optimized at the B3LYP level by using the standard LanL2DZ basis set and ECP for the $OsO_4 \cdot NH_3$ reactions.[19] The same basis set was used for the BNO and butadiene reactions for sake of consistency in all the calculations. All minima and transition structures were characterized by their vibrational frequences. All the reported thermodynamic data are given at 298.15 K from unscaled vibrational frequences in the harmonic approximation. Intrinsic reaction coordinate (IRC) calculations starting at the saddle points were carried out to check the connections between the transition structures, reactants and products.

Results and Discussion

Cycloadditions to 11

In analogy with the reactivity patterns of Diels–Alder reactions (normal, neutral and inverse)[20] the reactions of **11** with $OsO_4 \cdot NH_3$ belong to the inverse type, while the reactions with BNO and butadiene belong to the neutral and normal types, respectively, as shown by the frontier orbital (FO) energies and the global electrophilicity index ω[21] (Table 1). The global electrophilicity index ω is defined as

$\omega = \mu^2/2\eta$, where the chemical potential μ and the hardness η can be approximated as $\mu = (\varepsilon_{HOMO} + \varepsilon_{LUMO})/2$ and $\eta = (\varepsilon_{LUMO} - \varepsilon_{HOMO})$, and is a valuable descriptor of the reactivity of cycloadditions. The difference in the global electrophilicity index of the cycloaddends is related to the polar character of the mechanism.[22] In the cases at hand, only the cycloadditions of $OsO_4{\cdot}NH_3$ to **11** and **12** are expected to be significantly polar because of the large $\Delta\omega$ between the interacting pairs.

Table 1. FO energies [eV] and global electrophilicity ω [eV] for the cycloadditions of $OsO_4{\cdot}NH_3$, BNO and butadiene to olefin **11** and **12**.

	E_{HOMO}	E_{LUMO}	ω
$OsO_4{\cdot}NH_3$	–9.25	–4.68	5.32
BNO	–6.60	–1.77	1.81
Butadiene	–6.40	–0.97	1.25
11	–7.45	–0.84	1.30
12	–7.51	–1.11	1.45

We have located the *anti* and *syn* transition structures (TSs) of the cycloadditions of $OsO_4{\cdot}NH_3$, BNO and butadiene to **11** and the lowest TSs **13a**–**f** are displayed in Figure 2 along with the forming bonds, the tilting angles at the olefinic sites and the angles of attack to the olefin **11**.

A common feature of all the *anti* TSs is their early character as shown by the longer forming bonds with respect to the *syn* TSs. This is consistent with the idea that the GS *anti* pyramidalization of **11** indicates the direction of the easier facial distortion of the dipolarophiles in attaining the TS geometry. The *syn* addition requires more structural reorganization, resulting in later TSs. The earliness of the *anti* TS **13a** is remarkable in the addition of $OsO_4{\cdot}NH_3$, where the forming C···O bonds are longer by 0.15–0.19 Å than those of the *syn* TS **13b**. In the BNO TSs **13c**,**d**, the C···O bonds are still significantly different, while the difference between the C···C forming bonds is attenuated. In the butadiene TSs **13e**,**f** a smaller difference persists, and steric clashes show up in **13e** (wavy lines).

The thermodynamic data of TSs **13a**–**f** are reported in Table 2. The cycloadditions of BNO and butadiene show normal barriers, while the electronic and enthalpic activation barriers of the $OsO_4{\cdot}NH_3$ TSs are negative or slightly positive, and IRC calculations lead to lower-lying, floppy complexes **14a**,**b** on the side of reactants. The energies of the complexes are included in Table 2, and the geometries are given in the Supporting Information. On the free energy surface, complexes **14a**,**b** are above the addends and well below the cycloaddition TSs, so that their formation has no influence on the reaction pathway. The free energy activation barriers of all cycloadditions satisfactorily correspond to the experimental observations, and show a neat change going from a large *anti* preference (by 2.3 kcal/mol) with $OsO_4{\cdot}NH_3$ to a reduced *anti* preference (1.3 kcal/mol) with BNO and finally to a robust reversal with butadiene (*syn* preferred by 2.6 kcal/mol). Also given in the table are the natural bond orbital (NBO) charges transferred in the TSs and given as the charge resident on the olefin fragment

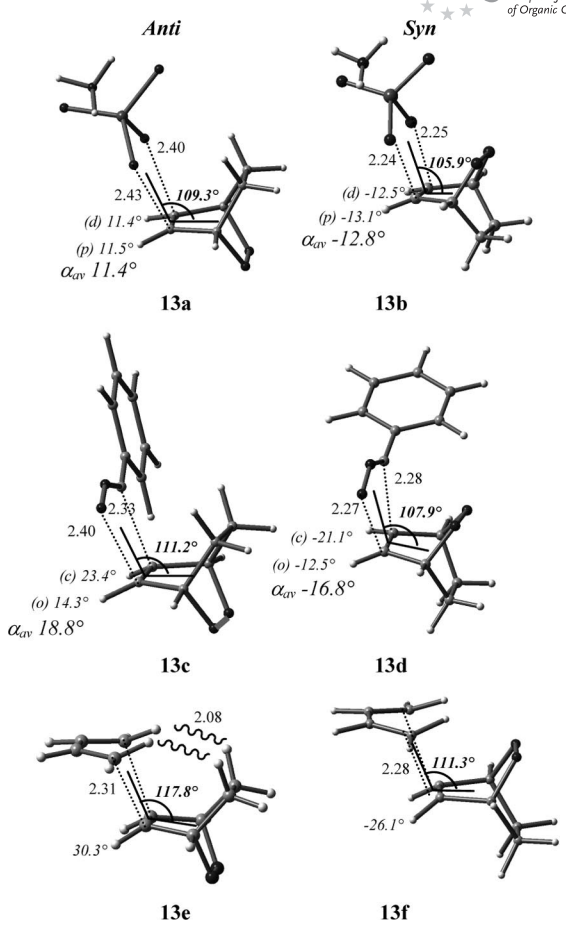

Figure 2. TSs **13a**–**f** of the cycloadditions of $OsO_4{\cdot}NH_3$, BNO and butadiene to **11**. Numbers near the forming bonds and steric clashes (wavy lines) specify bonding distances in Å. Numbers in italics near the vinyl hydrogen atoms are the tilting angles taken as positive and negative for *anti* and *syn* pyramidalization, respectively, while letters specify the location of the vinyl hydrogen atoms (p = proximal and d = distal to N in TSs **13a**,**b**; o and c near to the BNO O and C atoms in TSs **13c**,**d**). The average values (α_{av}) of the tilting angles are also given. Numbers in bold indicate the attacking angles Θ to **11**, defined as the angle between the olefin average plane C–C=C–C and the average plane defined by the four atoms connected by the forming bonds.

Table 2. Thermodynamic data for the TSs **13a**–**e** and the $OsO_4{\cdot}NH_3$ complexes **14a**,**b** relative to the addends. Relative energies are given in parentheses.

	$\Delta E^{\neq}$	$\Delta H^{\neq}$	$\Delta G^{\neq}$	Charge transfer[a]
$OsO_4{\cdot}NH_3$				
TS **13a**	–2.14 (0.0)	–0.95 (0.0)	9.03 (0.0)	0.157
TS **13b**	0.29 (2.43)	1.33 (2.27)	11.28 (2.25)	0.182
14a	–2.51	–0.71	5.43	
14b	–3.38	–1.58	4.62	
BNO				
TS **13c**	12.00 (0.0)	13.11 (0.0)	23.37 (0.0)	0.028
TS **13d**	13.29 (1.29)	14.21 (1.10)	24.62 (1.25)	0.007
Butadiene				
TS **13e**	26.60 (2.53)	27.98 (2.69)	38.63 (2.56)	–0.029
TS **13f**	24.07 (0.0)	22.59 (0.0)	36.07 (0.0)	–0.058

[a] NBO charge on olefin **11** in the TSs.

in the TSs. The cycloadditions of $OsO_4 \cdot NH_3$ to **11** are polar reactions and involve significant charge transfer from **11** to the more electrophilic osmium reagent. BNO cycloadditions do not show remarkable polarity, while in the butadiene cycloaddition, charge transfer takes place from butadiene to **11**, but only in a rather modest fashion because of the similar electrophilicities ω of the addends.

Table 3 gives an analysis of the activation barriers $\Delta E^{\neq}$ in terms of distortion energy (DE) and interaction energy (INT) according to the simple equation $\Delta E^{\neq}$ = DE + INT. DE is the energy required to distort the addends in the geometries they have in the TSs, and its role in affecting reactivity has been frequently discussed in the framework of Morokuma energy decomposition analysis.[23] INT refers to the interaction energy between the distorted addends, and takes into account contributions analogous to the familiar terms of the Klopman–Salem equation,[24] such as stabilizations due to filled- and unfilled-orbital interactions, closed-shell repulsion and Coulombic effects. The Klopman–Salem analysis was extensively applied in accounting for organic reactivity, and applies to the very early stages of the interactions between the orbitals of the undistorted reactants.[24] The availability of reliable TSs allows for a significant extension of the analysis to the TSs and the evaluation of the distortion of the reactants. The DIS/INT model has been recently applied by Ess and Houk to the reactivity of cycloaddition reactions, and allows for the assessment of the important role of distortion besides the interaction energy in determining the TSs.[25]

In applying the DIS/INT model to selectivity problems, the selectivity is given by $\Delta\Delta E^{\neq}$ = ΔDE + ΔINT, and two limiting cases can be envisaged: DE-controlled reactions where ΔDE >> ΔINT, and INT-controlled reactions in the opposite case. The data in Table 3 clearly show that the selectivity in osmilations is essentially due to the distortion of the olefin **11**. The $\Delta E^{\neq}$ barriers favour the *anti* TS **13a** by 2.4 kcal/mol, which turns out to be identical to the contribution of the DE of **11**, with only minor and opposing effects of the other contributors, i.e. DE(addend) (0.7) and INT (–0.7). In BNO cycloadditions, the DE(olefin) control lessens somewhat (2.0), and decreases further in butadiene cycloadditions (1.0). In the latter case, selectivity depends instead upon the INT term, which disfavours the *anti* approach.

Among the various factors affecting DA selectivities,[26] the origin of the switch to INT control in the case of butadiene can be easily traced to an overwhelming steric interaction between the facing CH bonds of butadiene and those of the dimethylene bridge of **11**, which show H···H contacts (2.08 Å) well below the sum of the van der Waals radii (2.20 Å). A visual comparison of the role of the various distortion and interaction effects is provided in Figure 3. On going to the right, the bold bars referring to the activation barriers $\Delta E^{\neq}$ change slope, pointing out the change

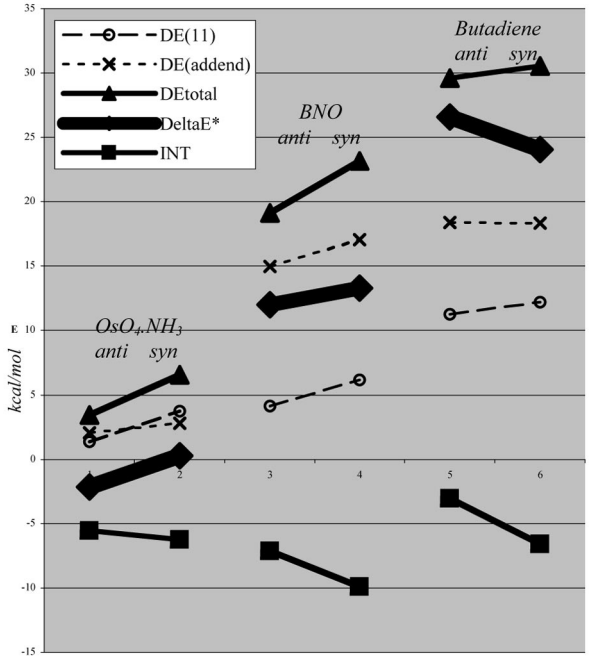

Figure 3. DIS/INT contributions to $\Delta E^{\neq}$ (bold bars) in the *anti* and *syn* cycloadditions to olefin **11**. Total DE values are given by the upper bars (triangles) and INT values by the lower bars (squares). The olefin DE values (open circles) and the addends DE values (cross) are shown by dashed and dotted bars, respectively.

Table 3. DE of olefin **11** (addends and total), activation energy $\Delta E^{\neq}$ and interaction energies INT of TS **13a**–**f** in kcal/mol. The selectivities $\Delta\Delta E^{\neq}$ and their contributors are given in parentheses.

TS	DE(**11**)	DE(addend)	DE_{Tot}	$\Delta E^{\neq}$	INT
$OsO_4 \cdot NH_3$					
13a	1.37 (0.0)	2.06 (0.0)	3.43 (0.0)	–2.14 (0.0)	–5.57 (0.0)
13b	3.76 (2.4)	2.80 (0.7)	6.56 (3.1)	0.29 (2.4)	–6.27 (–0.7)
BNO					
13c	4.15 (0.0)	14.97 (0.0)	19.12 (0.0)	12.00 (0.0)	–7.12 (2.8)
13d	6.16 (2.0)	17.03 (2.1)	23.19 (4.1)	13.29 (1.3)	–9.90 (0.0)
Butadiene					
13e	11.25 (0.0)	18.36 (0.0)	29.61 (0.0)	26.60 (2.5)	–3.01 (3.6)
13f	12.22 (1.0)	18.32 (0.0)	30.54 (0.9)	24.07 (0.0)	–6.57 (0.0)

in selectivity from *anti* to *syn*. The *anti* selectivity on the left stems almost exclusively from the olefin deformation as shown by the parallel bars of $\Delta E^{\neq}$ and DE(**11**). In the middle, the modest *anti* selectivity still derives from the deformation of the olefin, while DE(BNO) and INT are in opposition. On the right, the *syn* selectivity stems instead exclusively from the INT term, as show by the parallel bars of $\Delta E^{\neq}$ and INT.

Clearly, in the three reaction types discussed above, the DE control of olefin **11** on the *anti*/*syn* selectivity drops along the series, and the origin of this drop associated with the increase of total distortions and heights of the barriers is not immediately obvious. Figure 4 shows the change of the energy of **11** as a function of the tilting angle α of the vinyl hydrogen atoms. The minimum of the parabolic out-of-plane potential is located at α = +2.9°, and involves pyramidalization of the π orbital toward the *anti* space (arrow). Despite the almost negligible preference for the *anti* pyramidalization (0.11 kcal/mol with respect to the planar arrangement), the differences between the *anti* and *syn* deformations increase remarkably with increasing tilting angles. This is illustrated in the profile by the dotted lines, which connect the *syn* and *anti* points (diamond) with the same absolute values of α, and the number in parentheses on the left indicate the rising costs of the *syn* deformations with respect to the preferred *anti* ones on assuming similar tilting angles for *anti* and *syn* attack. The α angles derived from the olefin fragments of the TSs shown in Figure 2 indicate, however, that the tilts in the *syn* attack of **11** may be significantly less than in the *anti* attack, depending upon the addend.

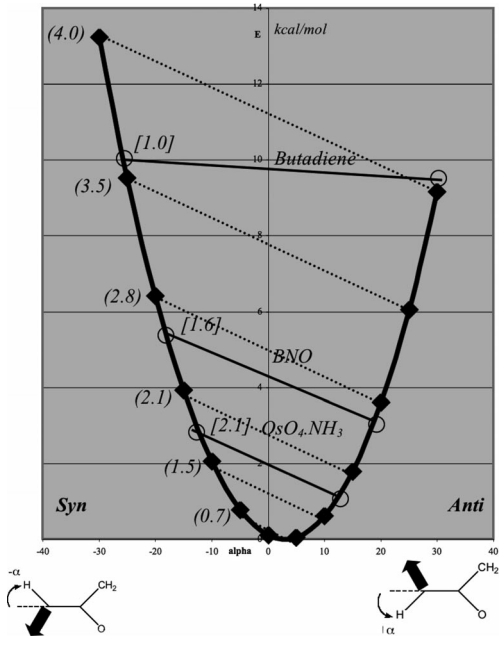

Figure 4. Out-of-plane potential of the olefin **11**. Bold arrows indicate the direction of pyramidalization of the π orbitals. Numbers in parentheses on the left give the energies [kcal/mol] of the *syn* deformations relative to the *anti* ones for the same absolute value of α. The open circles on the profile indicate the deformation energies corresponding to the α_{av} of the olefin in the TSs, and numbers in brackets indicate the *syn*/*anti* energy differences.

The energy corresponding to the average α angles of the olefin fragments in the TSs are indicated by the open circles on the parabolic potential in Figure 4, and the points belonging to the same reaction type are connected by full lines giving rise to a picture, which remarkably reproduces the drop of the DE control of selectivity due to the olefin deformation in osmilation (bottom), BNO cycloaddition (medium) and butadiene cycloaddition (top). The drop of the *syn*/*anti* energy differences at the α_{AV} values is given in brackets, and closely corresponds to the decrease of the relative values of DE(olefin) of Table 3.

The remarkably larger absolute values of the α angles for the *anti* attacks of butadiene can be related to the larger attacking angles Θ involved in the *anti* additions (see Figure 2). The severe steric hindrance between the facing hydrogen atoms enforces a large *anti* attacking angle Θ (117.8°), which in turn induces a large deformation in the olefin (α = 30.3°). In the *syn* addition, the attacking angle Θ is smaller (111.3°) and is associated with a smaller α (–26.1°). On going to BNO cycloadditions, the differential steric hindrance between the dimethylene bridge and the dihetero bridge attenuates, and the difference in $|\alpha|$ for the *anti* and *syn* attacks attenuates, too. In osmilations, the attacking angles Θ are comparable, as are the tilting angles $|\alpha|$, and the energetic effect of pyramidalization shows up entirely in the deformation energies. In summary, differences in attacking angle Θ affect the tilting angles of **11** and its deformation energies in a way, which offsets the natural predisposition of the pyramidalized olefin **11** to *anti* attack.

Cycloadditions to 12

The TSs **15a**–**f** of the cycloadditions to **12** have been located, and are shown in Figure 5. Analogous to the case of TSs **13a**–**f**, the *anti* TSs are earlier than the corresponding *syn* TSs, and the butadiene *anti* TS **15e** still shows slightly attenuated steric clashes between two hydrogen atoms of butadiene and the facing methylene hydrogen atom. The thermodynamic data are reported in Table 4, and in all cases, the barriers for the *anti* attack are remarkably lower than the *syn* ones, in keeping with the experimental trend. The $OsO_4 \cdot NH_3$ *anti* TS **15a** has negative electronic and enthalpic barriers, and could not be located in the usual way. Constrained optimizations along the approaching paths of the addends and frequency calculations on the optimized points of the reaction coordinate made it possible to identify the saddle on the free energy surface. The *syn* TS **15b** could be located in the usual way, and IRC calculations led to a loose complex **16b** similar to the complexes **14a**,**b** already discussed.

The DIS/INT analysis is given in Table 5, and a visual comparison of $\Delta E^{\neq}$ and its contributors is shown in Figure 6. The slopes of $\Delta E^{\neq}$ and DE(olefin) are alike, pointing

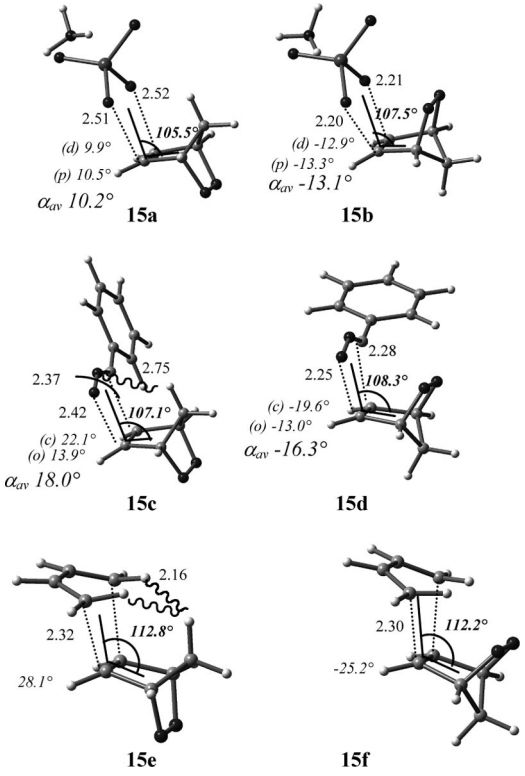

Figure 5. TSs **15a**–**f** of the cycloadditions of OsO_4·NH_3, BNO and butadiene to **12**. Numbers near the forming bonds and steric clashes (wavy lines) specify bonding distances in Å. Numbers in italics near the vinyl hydrogen atoms are the tilting angles taken as positive and negative for *anti* and *syn* pyramidalization, respectively. Letters specify the location of the vinyl hydrogen atoms (p = proximal and d = distal to N in TSs **15a**,**b**; o and c near the BNO O and C atoms in TSs **15c**,**d**). The average values (α_{av}) of the tilting angles are also given. Numbers in bold indicate the attacking angles Θ to **12**, defined as the angle between the olefin average plane C–C=C–C and the average plane defined by the four atoms connected by the forming bonds.

out that DE(olefin) is the more influential factor in determining the *anti* selectivity of these cycloadditions. Noteworthy is the opposing effect of INT, which disfavours the *anti* approach and reduces somewhat the role of DE(olefin)

Table 4. Thermodynamic data for the TSs **15a**–**e** and the OsO_4·NH_3 complexes **16b** relative to the addends. Relative energies are given in parentheses.

	$\Delta E^{\neq}$	$\Delta H^{\neq}$	$\Delta G^{\neq}$	Charge transfer[a]
OsO_4·NH_3				
TS **15a**	–3.26(0.00)	–2.08(0.00)	6.71 (0.00)	0.233
TS **15b**	2.74(6.00)	3.87(5.95)	14.02 (7.31)	0.135
16b	–3.38	–1.56	4.81	
BNO				
TS **15c**	9.42 (0.00)	10.42 (0.00)	20.13 (0.00)	0.015
TS **15d**	15.08 (5.65)	16.05 (5.63)	26.44 (6.31)	–0.012
Butadiene				
TS **15e**	21.96 (0.00)	23.16 (0.00)	33.67 (0.00)	–0.036
TS **15f**	24.96 (3.00)	26.20 (3.04)	36.96 (3.29)	–0.082

[a] NBO charge on olefin **12** in the TSs.

in the butadiene and also in the BNO cycloadditions. The INT effect can be attributed to the steric hindrance of the methylene bridge as shown in Figure 5 by the H···H and N···H contacts, which are slightly below the sum of the van der Waals radii. The steric hindrance of the methylene bridge is known to increase considerably upon methyl substitution, which leads eventually to a reversal of selectivity in cycloadditions to 7,7-dimethylnorbornene.[2]

Figure 7 shows the out-of-plane potential of olefin **12**. The parabolic potential is displaced at more positive values of α than that of **11**, and the minimum is located at α = +6.3°. The shift of the parabola to the right increases remarkably the differences between the *syn* and *anti* deformations with the same absolute values of α, enhancing the role of olefin distortions in determining cycloaddition selectivities, as shown by the *syn*/*anti* energy differences given at the left in parentheses. Differences in the attacking angles may cause here only a moderate erosion of the DE(olefin) control of selectivity. The energies corresponding to the average α angles of the olefin fragments in the TSs are shown by the open circles on the parabolic potential, and their *syn*/*anti* differences (given in brackets) correspond well to the relative DE(olefin) values given in Table 5.

Table 5. DE of olefin **12** (addends and total), activation energy $\Delta E^{\neq}$ and interaction energies INT of TSs **15a**–**f** in kcal/mol. The selectivities $\Delta\Delta E_{el}^{\neq}$ and their contributors are given in parentheses.

TS	DE(**12**)	DE(addend)	DE_{Tot}	$\Delta E^{\neq}$	INT
OsO_4·NH_3					
15a	0.45 (0.00)	1.16 (0.00)	1.67 (0.00)	–3.26 (0.00)	–4.93 (0.00)
15b	5.92 (5.47)	3.04 (1.88)	8.96 (7.29)	2.74 (6.00)	–6.22 (–1.29)
BNO					
15c	2.58 (0.00)	13.54 (0.00)	16.12 (0.00)	9.42 (0.00)	–6.70 (3.00)
15d	7.99 (5.30)	16.75 (3.20)	24.74 (8.60)	15.08 (5.70)	–9.66 (0.00)
Butadiene					
15e	7.96 (0.00)	17.15 (0.00)	25.11 (0.00)	21.96 (0.00)	–3.15 (3.80)
15f	14.69 (6.70)	17.24 (0.10)	31.93 (6.80)	24.96 (3.32)	–6.97 (0.00)

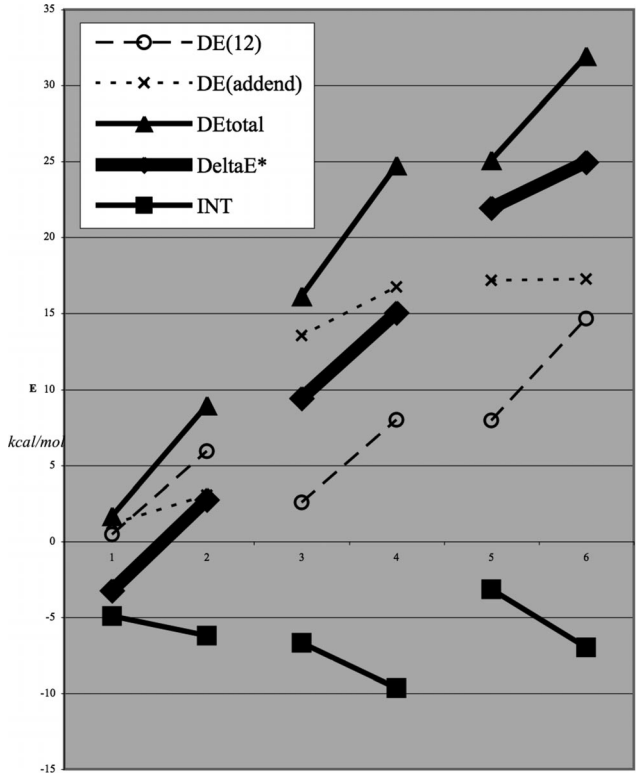

Figure 6. DIS/INT contributions to $\Delta E^{\neq}$ (bold bars) in the *anti* and *syn* cycloadditions to olefin **12**. Total DE values are given by the upper bars (triangles) and INT values by the lower bars (squares). The olefin DE values (open circles) and the addend DE values (crosses) are shown by dashed and dotted bars, respectively.

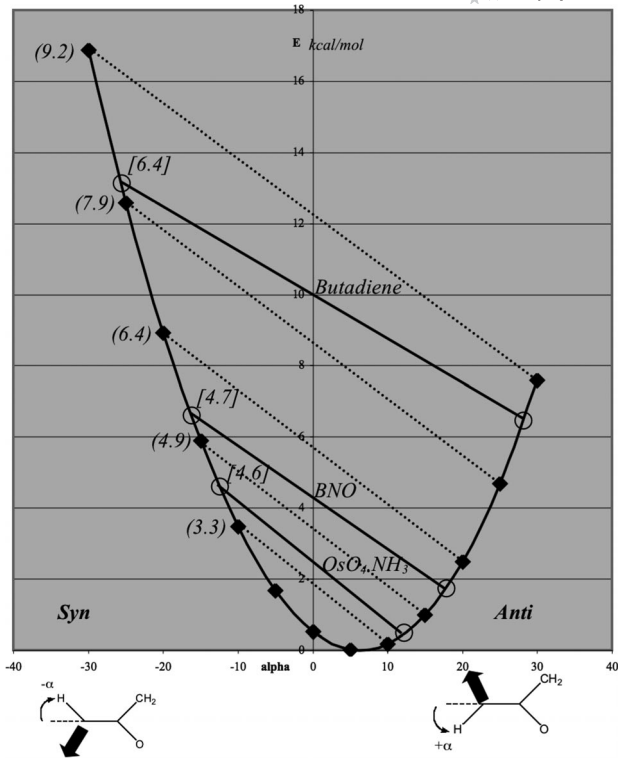

Figure 7. Out-of-plane potential of the olefin **12**. Numbers in parentheses on the left give the energies [kcal/mol] of the *syn* deformations relative to the *anti* ones for the same absolute value of *a*. The open circles on the profile indicate the deformation energies corresponding to the a_{av} of the olefin in the TSs, and numbers in brackets indicate the *syn*/*anti* energy differences.

Summary and Conclusions

The 2,3-dioxa and 2-oxa-3-azabicyclo[2.2.2]octenes **11** and **1b** show modest deformation of the double bonds because of the conflicting effects of the π/σ and π/σ* allylic interactions. The latter interactions are more influential, and cause pyramidalization of the olefinic carbon atoms towards the *anti* space implying easier *anti* additions. The natural predisposition to *anti* additions may be offset by the mutual interactions between the addends. In the cases at hand, the steric hindrance of the dimethylene bridge is larger than that of the dihetero bridge, and constrains bulky reactants to adopt larger attacking angles when approaching on the side of the dimethylene bridge, i.e. *anti* to the dihetero bridge. The larger *anti* attacking angles induce a higher olefin distortion and an increase of the out-of-plane tilting angles at the vinyl centers as exemplified in Figure 8.

The energetically costly increase of the tilting angles in the *anti* attack counteracts the natural predisposition to *anti* additions of these olefins, and reduces the DE(olefin) control of selectivity. In the case of butadiene cycloadditions, the unfavourable steric interactions between the addends is only in part relieved by increasing the *anti* attacking angle, which remarkably dampens the DE(olefin) control. The residual part of the steric effect shows up in the INT term and disfavours the *anti* attack leading to a neat reversal of selectivity.

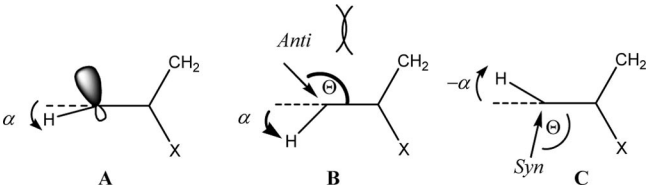

Figure 8. Ground-state pyramidalization *anti* to the dihetero bridge of bicyclo derivatives **11** and **12** (A). Steric interactions between the addends widens the attacking angle *Θ* and the tilting angle *α* in the *anti* addition (B) with respect to the *syn* additions (C).

The 2,3-dioxa- and 2-oxa-3-azabicyclo[2.2.1]heptenes **12** and **1a** show larger pyramidalizations because of the cooperating π/σ and π/σ* interactions. This results in a remarkably higher predisposition to *anti* additions, similar to the strict *exo* preference of norbornene. Mutual interactions cannot efficiently compete with the rigid *anti* predisposition in these cases and have only a subordinate influence on selectivities.

In summary, steric interactions between the addends affect the distortive ability of pyramidalized olefins and represent a sound alternative to the controversial Cieplak TS effect. We surmise that the "*syn* oxygen phenomenon"[14] observed in cycloadditions of dienes to cyclic alkenes containing geminal allylic alkyl and alkoxy substituents can be similarly accounted for by the different steric hindrance and

distortions in the *syn* and *anti* addition shown in Figure 8. The preference for the *syn* oxygen addition can then be attributed to reduced steric hindrance on the oxygen side and to the smaller olefin distortion involved.

Thus, we have addressed by quantum chemical calculations the puzzling issue of facial selectivity in a few cycloadditions possessing some synthetic, biological and pharmaceutical potential. Calculations have shed some light on the delicate interplay of various electronic and steric factors, and correctly interpret experimental results.

Supporting Information (see footnote on the first page of this article): Cartesian coordinates of addends and cycloaddition TSs.

Acknowledgments

Financial support by the University of Pavia (FAR) and the Ministero dell'Università e della Ricerca (MIUR) (PRIN2008) is gratefully acknowledged. A research grant by the Fondazione Banca del Monte di Lombardia is also gratefully acknowledged. Allocations of computer time by CINECA (Centro Interuniversitario Nord-Est di Calcolo Automatico, Casalecchio di Reno, Bologna) as well as by CASPUR (Consorzio Interuniversitario per le Applicazioni di Supercalcolo per Università e Ricerca, Rome) are also gratefully acknowledged.

[1] a) P. F. Vogt, M. J. Miller, *Tetrahedron* **1998**, *54*, 1317–1348; b) L. Boger, S. M. Weinreb, *Hetero Diels–Alder Methodology in Organic Synthesis*, Academic Press, San Diego, **1987**; c) A. Miller, G. Procter, *Tetrahedron Lett.* **1990**, *31*, 1043–1046; d) G. W. Kirby, M. Nazeer, *J. Chem. Soc. Perkin Trans. 1* **1993**, 1397–1402; e) V. Gouverneur, S. J. McCarthy, C. Mineur, D. Belotti, G. Dive, L. Ghosez, *Tetrahedron* **1998**, *54*, 10537–10554; f) G. Calvet, M. Dussaussois, N. Blanchard, C. Kouklovsky, *Org. Lett.* **2004**, *6*, 2449–2451 and references cited therein; g) S. Iwasa, A. Fakhruddin, H. Nishiyama, *Mini-Rev. Org. Chem.* **2005**, *2*, 157–175.

[2] J. Freeman, *Chem. Rev.* **1975**, *75*, 439–489.

[3] G. Mehta, J. Chandrasekhar, *Chem. Rev.* **1999**, *99*, 1437–1467.

[4] R. Huisgen, P. H. J. Ooms, M. Mingin, N. L. Allinger, *J. Am. Chem. Soc.* **1980**, *102*, 3951–3953.

[5] N. G. Rondan, M. N. Paddon-Row, P. Caramella, K. N. Houk, *J. Am. Chem. Soc.* **1981**, *103*, 2436–2438.

[6] a) P. Caramella, N. G. Rondan, M. N. Paddon-Row, K. N. Houk, *J. Am. Chem. Soc.* **1981**, *103*, 2438–2440; b) K. N. Houk, N. G. Rondan, F. K. Brown, W. L. Jorgensen, J. D. Madura, D. C. Spellmeyer, *J. Am. Chem. Soc.* **1983**, *105*, 5980–5988.

[7] a) S. Ranganathan, K. S. George, *Tetrahedron* **1997**, *53*, 3347–3362; b) M. Cowart, M. J. Bennett, J. F. Kerwin Jr., *J. Org. Chem.* **1999**, *64*, 2240–2249; c) B. T. Shireman, M. J. Miller, *Tetrahedron Lett.* **2000**, *41*, 9537–9540; d) K.-H. Kim, M. J. Miller, *Tetrahedron Lett.* **2003**, *44*, 4571–4573.

[8] P. Quadrelli, M. Mella, P. Paganoni, P. Caramella, *Eur. J. Org. Chem.* **2000**, 2613–2620.

[9] H. Noguchi, T. Aoyama, T. Shioiri, *Heterocycles* **2002**, *58*, 471–504.

[10] a) D. L. Boger, M. Patel, F. Takusagawa, *J. Org. Chem.* **1985**, *50*, 1911–1916; b) D. L. Boger, M. Patel, *Tetrahedron Lett.* **1986**, *27*, 683–686.

[11] P. Quadrelli, M. Mella, S. Carosso, B. Bovio, P. Caramella, *Eur. J. Org. Chem.* **2007**, 6003–6015.

[12] B. S. Bodnar, M. J. Miller, *J. Org. Chem.* **2007**, *72*, 3929–3932.

[13] a) A. S. Cieplak, B. D. Tait, C. R. Johnson, *J. Am. Chem. Soc.* **1989**, *111*, 8447–8462; b) H. Li, W. J. le Noble, *Recl. Trav. Chim. Pays-Bas* **1992**, *111*, 199–210; c) A. S. Cieplak, *Chem. Rev.* **1999**, *99*, 1265–1336; d) M. Kaselj, W.-S. Chung, W. J. le Noble, *Chem. Rev.* **1999**, *99*, 1387–1413.

[14] K. Ohkata, Y. Tamura, B. B. Shetuni, R. Takagi, W. Miyanaga, S. Kojima, L. A. Paquette, *J. Am. Chem. Soc.* **2004**, *126*, 16783–16792 and references cited therein.

[15] J. J. Dannenberg, *Chem. Rev.* **1999**, *99*, 1225–1242.

[16] a) P. Valente, T. D. Avery, D. K. Taylor, E. R. T. Tiekink, *J. Org. Chem.* **2009**, *74*, 274–282; b) R. Gandolfi, G. Tonoletti, A. Rastelli, M. Bagatti, *J. Org. Chem.* **1993**, *58*, 6038–6048.

[17] A. J. Bloodworth, W. J. Eggelte, *J. Chem. Soc. Perkin Trans. 2* **1984**, 2069–2072.

[18] M. J. Frisch, G. W. Trucks, H. B. Schlegel, G. E. Scuseria, M. A. Robb, J. R. Cheeseman, J. A. Montgomery Jr., T. Vreven, K. N. Kudin, J. C. Burant, J. M. Millam, S. S. Iyengar, J. Tomasi, V. Barone, B. Mennucci, M. Cossi, G. Scalmani, N. Rega, G. A. Petersson, H. Nakatsuji, M. Hada, M. Ehara, K. Toyota, R. Fukuda, J. Hasegawa, M. Ishida, T. Nakajima, Y. Honda, O. Kitao, H. Nakai, M. Klene, X. Li, J. E. Knox, H. P. Hratchian, J. B. Cross, C. Adamo, J. Jaramillo, R. Gomperts, R. E. Stratmann, O. Yazyev, A. J. Austin, R. Cammi, C. Pomelli, J. W. Ochterski, P. Y. Ayala, K. Morokuma, G. A. Voth, P. Salvador, J. J. Dannenberg, V. G. Zakrzewski, S. Dapprich, A. D. Daniels, M. C. Strain, O. Farkas, D. K. Malick, A. D. Rabuck, K. Raghavachari, J. B. Foresman, J. V. Ortiz, Q. Cui, A. G. Baboul, S. Clifford, J. Cioslowski, B. B. Stefanov, G. Liu, A. Liashenko, P. Piskorz, I. Komaromi, R. L. Martin, D. J. Fox, T. Keith, M. A. Al-Laham, C. Y. Peng, A. Nanayakkara, M. Challacombe, P. M. W. Gill, B. Johnson, W. Chen, M. W. Wong, C. Gonzalez, J. A. Pople, *Gaussian 03*, Revision B.02, Gaussian, Inc., Pittsburgh, PA, **2003**.

[19] D. H. Ess, *J. Org. Chem.* **2009**, *74*, 1498–1508.

[20] a) J. Sauer, R. Sustmann, *Angew. Chem. Int. Ed. Engl.* **1980**, *19*, 779–807; b) W. Oppolzer, in *Comprehensive Organic Synthesis* (Ed.: L. A. Paquette), Pergamon Press, Oxford, **1991**, vol. 5, pp. 315–399.

[21] a) P. K. Chattaraj, U. Sarkar, D. R. Roy, *Chem. Rev.* **2006**, *106*, 2065–2091; b) D. H. Ess, G. O. Jones, K. N. Houk, *Adv. Synth. Catal.* **2006**, *348*, 2337–2361.

[22] L. R. Domingo, M. J. Aurell, P. Perez, R. Contreras, *Tetrahedron* **2002**, *58*, 4417–4423; a) P. Perez, L. R. Domingo, M. J. Aurell, R. Contreras, *Tetrahedron* **2003**, *59*, 3117–3125; b) M. J. Aurell, L. R. Domingo, P. Perez, R. Contreras, *Tetrahedron* **2004**, *60*, 11503–11509.

[23] a) K. Morokuma, *Acc. Chem. Res.* **1977**, *10*, 284–300; b) F. M. Bickelhaupt, E. J. Baerends, *Rev. Comput. Chem.* **2000**, *15*, 1–86; c) K. N. Houk, J. C. Williams, P. A. Mitchell, K. Yamaguchi, *J. Am. Chem. Soc.* **1981**, *103*, 949–951.

[24] a) I. Fleming, *Frontier Orbitals and Organic Chemical Reactions*, J. Wiley and Sons, London, **1976**, p. 27; b) G. Klopman, *J. Am. Chem. Soc.* **1968**, *90*, 223–234; c) L. Salem, *J. Am. Chem. Soc.* **1968**, *90*, 543–552; L. Salem, *J. Am. Chem. Soc.* **1968**, *90*, 553–566.

[25] a) D. H. Ess, K. N. Houk, *J. Am. Chem. Soc.* **2007**, *129*, 10646–10647; b) D. H. Ess, K. N. Houk, *J. Am. Chem. Soc.* **2008**, *130*, 10187–10198.

[26] For a critical overview see: a) J. I. Garcia, J. A. Mayoral, L. Salvatella, *Acc. Chem. Res.* **2000**, *33*, 658–664; b) J. I. Garcia, J. A. Mayoral, L. Salvatella, *Eur. J. Org. Chem.* **2005**, 85–90.

Received: May 20, 2010
Published Online: October 28, 2010

